6 Modeling Synapses

Arnd Roth and Mark C. W. van Rossum

Modeling synaptic transmission between neurons is a challenging task. Since many physiological processes contribute to synaptic transmission (figure 6.1), computational models require numerous simplifications and abstractions. Furthermore, since synapses change their properties on many time scales, synaptic transmission is also a highly dynamic process. In addition, synaptic transmission is stochastic and believed to be an important source of noise in the nervous system. Finally, because the number of synapses in any decent-sized network is large (chapter 13), efficient simulation routines are important.

The human brain is estimated to contain some 10^{14} synapses. Even if all synapses were identical, modeling them would present a substantial computational challenge. Moreover, synaptic connections in the central nervous system are highly diverse. This diversity is not simply due to random variability, but most likely reflects a highly specified and precise design. For example, the same presynaptic axon can give rise to synapses with different properties, depending on the type of the postsynaptic target neuron (Thomson et al., 1993; Thomson, 1997; Reyes et al., 1998; Markram et al., 1998). At the same time, synapses on a given postsynaptic dendrite can have different properties, depending on their dendritic location and the identity of the presynaptic neuron (Walker et al., 2002).

Moreover, synaptic efficacies are not static but have activity-dependent dynamics in the form of short-term (Zucker and Regehr, 2002) and long-term plasticity (Abbott and Nelson, 2000), which are the consequence of complex molecular networks. Simulation of synaptic transmission therefore requires careful simplifications. This chapter describes models at different levels of realism and computational efficiency for simulating synapses and their plasticity. We also review experimental data that provide the parameter values for the synapse models, focusing on the dominant transmitter and receptor types mediating fast synaptic transmission in the mammalian central nervous system.

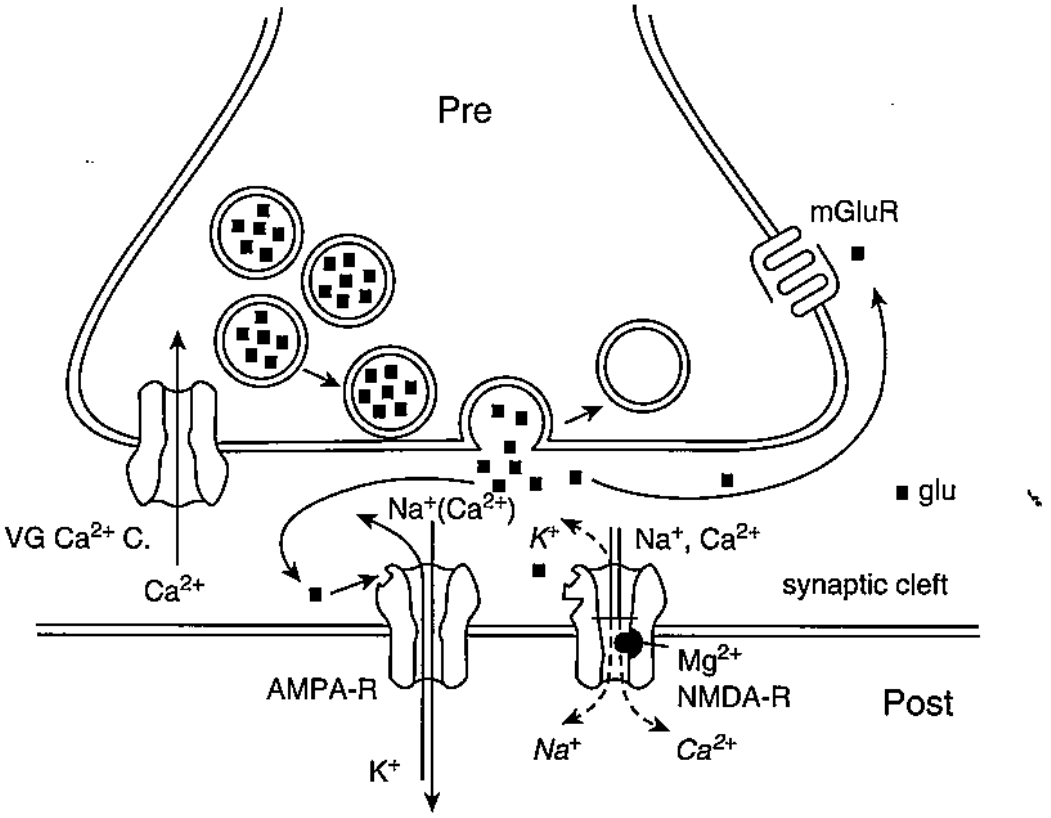

Figure 6.1
Overview of glutamergic synaptic transmission. Schematic illustrating the signaling cascade underlying synaptic transmission. In response to a presynaptic action potential, calcium enters the presynaptic terminal via voltage-gated calcium channels (VG Ca^{2+} C.) and triggers the release of glutamate-containing vesicles. Glutamate diffuses into the synaptic cleft and activates postsynaptic AMPA and NMDA receptors (R), ionotropic receptors that act via opening of an ion channel permeable to sodium, potassium, and calcium, giving rise to a fast excitatory postsynaptic current (EPSC). Glutamate can also activate pre- and postsynaptic metabotropic glutamate receptors (mGluRs), which act via G-proteins. (Drawing by Henrik Alle, reproduced with permission.)

6.1 Simple Models of Synaptic Kinetics

The basic mechanism of synaptic transmission is well established: a presynaptic spike depolarizes the synaptic terminal, leading to an influx of calcium through presynaptic calcium channels, causing vesicles of neurotransmitter to be released into the synaptic cleft. The neurotransmitter binds temporarily to postsynaptic channels, opening them and allowing ionic current to flow across the membrane. Modeling this complete process is rather challenging (see sections 6.3–6.5); however, many simple phenomenological models of synapses can represent the time and voltage dependence of synaptic currents fairly well (figure 6.2).

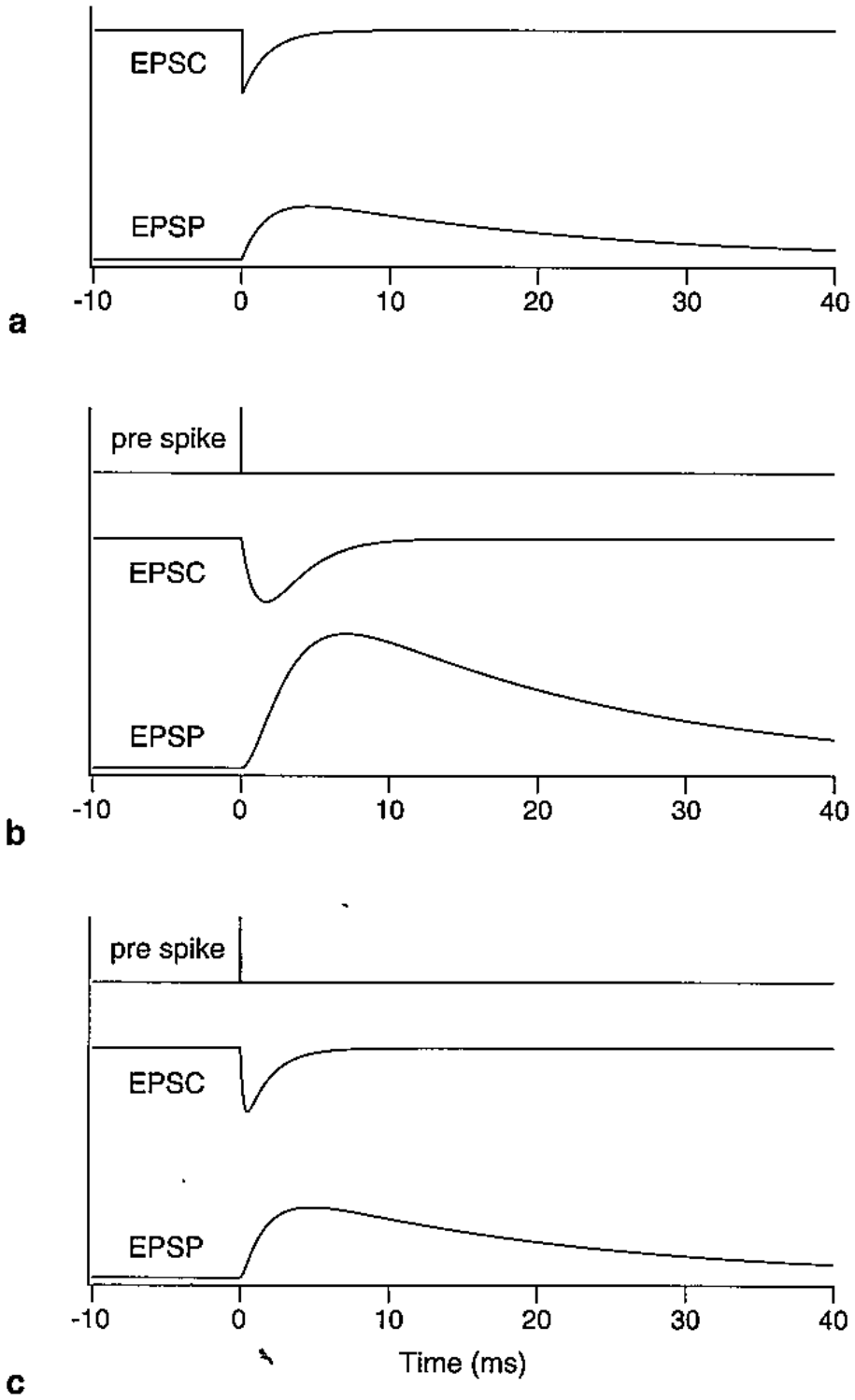

Figure 6.2
Sequence of events in simple models of synaptic kinetics. Panels a–c show the time of the presynaptic spike (top), the time course of the excitatory postsynaptic current (EPSC, middle), and the time course of the resulting postsynaptic membrane depolarization or excitatory postsynaptic potential (EPSP, bottom) for three simple models of the synaptic conductance. (a) Instantaneous rise and single-exponential decay (equation 6.1, $\tau = 1.7$ ms). (b) Alpha function (equation 6.3, $\tau = 1.7$ ms). (c) Difference of two exponentials (equation 6.4, $\tau_{rise} = 0.2$ ms, $\tau_{decay} = 1.7$ ms). The EPSC, which is negative by convention (equation 6.10), charges the membrane capacitance, leading to a transient postsynaptic depolarization whose rise time depends mainly on the kinetics of the EPSC and whose decay time constant is dominated by the postsynaptic membrane time constant. The peak synaptic conductance, postsynaptic input resistance, and membrane time constant (20 ms) were the same for all three models. EPSPs are shown for a single-compartment postsynaptic neuron. If the synapse is located on a dendrite distant from the soma, as is common, filtering by the dendritic cable will reduce the amplitude and prolong the time course of the somatic EPSP (chapter 10, section 3).

Instantaneous Rise and Single-Exponential Decay

One of the simplest and often-used models assumes an instantaneous rise of the synaptic conductance $g_{\text{syn}}(t)$ from 0 to $\bar{g}_{\text{syn}}$ (the peak conductance) at time t_0 followed by an exponential decay with a time constant τ (figure 6.2a):

$$g_{\text{syn}}(t) = \bar{g}_{\text{syn}} e^{-(t-t_0)/\tau}. \tag{6.1}$$

For times $t < t_0$ before the onset of the synaptic conductance, $g_{\text{syn}}(t) = 0$. The time t_0 is the time of the presynaptic spike, or more realistically, a transmission delay can be included (see section 6.2).

A possible justification for this simple model is as follows: Suppose one has a large number of two-state synaptic channels. Now assume that the release of neurotransmitter, its diffusion across the cleft, the receptor binding, and channel opening all happen very quickly, so that the channels instantaneously jump from the closed to the open state. The transmitter transient disappears quickly and the open probability, and hence the conductance, decay exponentially as the channels make transitions back into the closed state. The corresponding differential equation is

$$\tau \frac{dg_{\text{syn}}(t)}{dt} = -g_{\text{syn}}(t) + \bar{g}_{\text{syn}} \delta(t_0 - t), \tag{6.2}$$

where $\delta(t)$ is the Dirac delta function. The decay time constant τ is largely determined by the unbinding of the neurotransmitter from the receptor channel. In particular for certain types of inhibitory postsynaptic currents (IPSCs), the exponential synapse is a good approximation because the rising phase is much shorter than their decay phase (e.g., Kraushaar and Jonas, 2000), but also for fast AMPA-mediated excitatory postsynaptic currents (EPSCs), it is a decent model.

Alpha Function

However, for most synapses, the rising phase of synaptic conductances has a finite duration, which can have strong effects on network dynamics (van Vreeswijk et al., 1994). The so-called alpha function describes a conductance that has a rising phase that is not infinitely fast, but has a certain rise time (figure 6.2b):

$$g_{\text{syn}}(t) = \bar{g}_{\text{syn}} \frac{t - t_0}{\tau} e^{1-(t-t_0)/\tau}. \tag{6.3}$$

However, because it has just a single time constant, τ, the time courses of the rise and decay are correlated and cannot be set independently. In general this condition is not physiologically realistic; nevertheless the alpha function provides a reasonable approximation for some synapses. It peaks at a time $t - t_0 = \tau$, and for the above definition the peak amplitude is given directly by $\bar{g}_{\text{syn}}$. As before, $g_{\text{syn}}(t) = 0$ for $t < t_0$.

Difference of Two Exponentials

A more general function describing synaptic conductance profiles consists of a difference of two exponentials, one for the rising and one for the decay phase. It allows these time constants to be set independently ($\tau_{\text{rise}} \neq \tau_{\text{decay}}$), so that for $t \geq t_0$ (figure 6.2c):

$$g_{\text{syn}}(t) = \bar{g}_{\text{syn}} f (e^{-(t-t_0)/\tau_{\text{decay}}} - e^{-(t-t_0)/\tau_{\text{rise}}}). \tag{6.4}$$

The normalization factor f is included to ensure that the amplitude equals $\bar{g}_{\text{syn}}$. The conductance peaks at a time:

$$t_{\text{peak}} = t_0 + \frac{\tau_{\text{decay}}\tau_{\text{rise}}}{\tau_{\text{decay}} - \tau_{\text{rise}}} \ln\left(\frac{\tau_{\text{decay}}}{\tau_{\text{rise}}}\right), \tag{6.5}$$

and the normalization factor for the amplitude follows as

$$f = \frac{1}{-e^{-(t_{\text{peak}}-t_0)/\tau_{\text{rise}}} + e^{-(t_{\text{peak}}-t_0)/\tau_{\text{decay}}}}. \tag{6.6}$$

In the case of most synapses, rapid binding is followed by slow unbinding of the transmitter. This particular profile of the synaptic conductance can be interpreted as the solution of two coupled linear differential equations (Wilson and Bower, 1989; Destexhe et al. 1994):

$$g_{\text{syn}}(t) = \bar{g}_{\text{syn}} f g(t) \tag{6.7}$$

$$\frac{dg}{dt} = -\frac{g}{\tau_{\text{decay}}} + h \tag{6.8}$$

$$\frac{dh}{dt} = -\frac{h}{\tau_{\text{rise}}} + h_0 \delta(t_0 - t), \tag{6.9}$$

with h_0 a scaling factor. The alpha function is retrieved in the limit when both time constants are equal.

The time course of most synaptic conductances can be well described by this difference of two exponentials. It is of course possible to further increase the number of exponentials describing the synaptic conductance to obtain even better fits, but then no closed-form expression for the time of peak and the normalization factor for the amplitude exists. Furthermore, extracting a large number of exponentials from noisy data is cumbersome (see later discussion).

Conductance-Based and Current-Based Synapses

Most ligand-gated ion channels mediating synaptic transmission, such as AMPA-type glutamate receptors and γ-aminobutryic acid type A ($GABA_A$) receptors (see

section 6.3), display an approximately linear current-voltage relationship when they open. They can therefore be modeled as an ohmic conductance g_{syn} which when multiplied with the driving force, the difference between the membrane potential V and the reversal potential E_{syn} of the synaptic conductance, gives the synaptic current

$$I_{syn} = g_{syn}(t)[V(t) - E_{syn}]. \tag{6.10}$$

However, in some cases, in particular in analytical models, it may be a useful approximation to consider synapses as sources of current and not a conductance, i.e., without the dependence on the membrane potential V as described by equation (6.10). This can be achieved, for example, by using a fixed value $V = V_{rest}$ in equation (6.10). For small excitatory synapses on a large compartment, this is a good approximation. In that case, the depolarization of the membrane will be small and hence the difference between V and E_{syn} will hardly change during the excitatory postsynaptic potential (EPSP). However, if the synapse is located on a thin dendrite, the local membrane potential V changes considerably when the synapse is activated (Nevian et al., 2007). In that case a conductance-based synapse model seems more appropriate. Nevertheless, voltage-dependent ion channels in the dendritic membrane, together with a voltage-dependent component in the synaptic conductance g, mediated by NMDA receptors (see next), can at least partially compensate for the change in membrane potential and can cause synapses to effectively operate as current sources (Cook and Johnston, 1999).

For inhibitory synapses, the distinction between conductance-based and current-based models is particularly important because the inhibitory reversal potential can be close or even above the resting potential. As a result, the resulting synaptic current becomes highly dependent on the postsynaptic voltage. This shunting leads to shortening of the membrane time constant, which does not occur for current-based models. This can have substantial consequences for network simulations (Koch, 1999; Vogels and Abbott, 2005; Kumar et al., 2008; chapter 13, section 7).

Simple Descriptions of NMDA Receptor-Mediated Synaptic Conductances

Excitatory synaptic currents commonly have both AMPA and NMDA components. The NMDA current is mediated by NMDA channels, which like AMPA channels, are activated by glutamate but have a different sensitivity. The NMDA receptor-mediated conductance depends on the postsynaptic voltage, i.e., equation (6.10) is not valid. The voltage dependence is due to the blocking of the pore of the NMDA receptor from the outside by a positively charged magnesium ion. The channel is nearly completely blocked at resting potential, but the magnesium block is relieved if the cell is depolarized. The fraction of channels $u(V)$ that are not blocked by magnesium can be fitted to

$$u(V) = \frac{1}{1 + e^{-aV}[\mathrm{Mg}^{2+}]_o/b}, \tag{6.11}$$

with $a = 0.062\ \mathrm{mV}^{-1}$ and $b = 3.57$ mM (Jahr and Stevens, 1990). Here $[\mathrm{Mg}^{2+}]_o$ is the extracellular magnesium concentration, usually 1 mM. If we make the approximation that the magnesium block changes instantaneously with voltage and is independent of the gating of the channel, the net NMDA receptor-mediated synaptic current is given by

$$I_{\mathrm{NMDA}} = g_{\mathrm{NMDA}}(t)u(V)[V(t) - E_{\mathrm{NMDA}}], \tag{6.12}$$

where $g_{\mathrm{NMDA}}(t)$ could for instance be modeled by a difference of exponentials, equation (6.4). Thus NMDA receptor activation requires both presynaptic activity (to provide glutamate) and postsynaptic activity (to release the magnesium block). This property has wide implications for the functional role of NMDA receptors for synaptic integration (Schiller et al., 2000; Losonczy and Magee, 2006; Nevian et al., 2007), neuronal excitability (Rhodes and Llinás, 2001), network dynamics (Compte, 2006; Durstewitz and Seamans, 2006; Durstewitz and Gabriel, 2007) and synaptic plasticity (Bliss and Collingridge, 1993).

Finally, NMDA receptors have a significant permeability for calcium ions and constitute one of the pathways for calcium entry, which is relevant for synaptic plasticity (Nevian and Sakmann, 2006). To calculate the calcium current through the NMDA receptor, the Goldman-Hodgkin-Katz equation should be used (see equation 4.2 and Badoual et al., 2006).

Synaptic Time Constants for AMPA, NMDA, and $\mathrm{GABA_A}$

The time constants of synaptic conductances vary widely among synapse types. However, some general trends and typical values can be identified. First, synaptic kinetics tends to accelerate during development (T. Takahashi, 2005). Second, synaptic kinetics becomes substantially faster with increasing temperature. In the following discussion, we therefore focus on data from experiments performed at near-physiological temperature (34–38 °C). This is important because the temperature dependence is different for the various processes involved in synaptic transmission (transmitter diffusion, receptor kinetics, single channel conductance, etc.). In analogy with voltage-gated channels, the temperature dependence can be approximated with a Q_{10} factor, which describes the speedup with every 10 degrees of temperature increase (equation 5.43). In particular, the temperature dependence of synaptic kinetics is generally steep, with a Q_{10} of typically around 2–3 (Huntsman and Huguenard, 2000; Postlethwaite et al., 2007). Further complication arises because the Q_{10} of the different transitions in the state diagram can vary (e.g., Cais et al., 2008), so that a uniform scaling of all time constants is not appropriate.

AMPA receptor-mediated EPSCs at glutamatergic synapses are among the fastest synaptic currents, but because different types of neurons express different subtypes of AMPA receptors (see section 6.3), a range of time constants is observed. The fastest AMPA receptor-mediated EPSCs are found in the auditory system where $\tau_{decay} = 0.18$ ms in the chick nucleus magnocellularis (Trussell, 1999). Excitatory synapses onto interneurons in the cortex and hippocampus also tend to have a fast AMPA component ($\tau_{rise} = 0.25$ ms and $\tau_{decay} = 0.77$ ms in dentate gyrus basket cells; Geiger et al., 1997). Synapses onto pyramidal neurons tend to have slower AMPA components ($\tau_{rise} = 0.2$ ms and $\tau_{decay} = 1.7$ ms in neocortical layer 5 pyramidal neurons; Häusser and Roth, 1997b).

The NMDA receptor-mediated component of the EPSC is typically more than an order of magnitude slower than the AMPA receptor-mediated component. The slow unbinding rate of glutamate from the NMDA receptor makes NMDA more sensitive to glutamate and causes glutamate to stick longer to the receptor, increasing the open time. The decay time constants at near-physiological temperature range from 19 ms in dentate gyrus basket cells (Geiger et al., 1997) to 26 ms in neocortical layer 2/3 pyramidal neurons (Feldmeyer et al., 2002), and up to 89 ms in CA1 pyramidal cells (Diamond, 2001). Likewise NMDA rise times, which are about 2 ms (Feldmeyer et al., 2002), are slower than AMPA rise times. The reversal potential of both AMPA and NMDA receptor-mediated currents is, conveniently, around 0 mV under physiological conditions.

Synapses often contain both AMPA and NMDA receptor-mediated conductances in a specific ratio (Feldmeyer et al., 2002; Losonczy and Magee, 2006). However, there are also NMDA receptor-only synapses, so-called silent synapses (Liao et al., 1995; Isaac et al., 1995; Groc et al., 2006). These have little or no synaptic current at the resting potential because the NMDA receptors are blocked by magnesium. A few types of synapses are AMPA receptor-only synapses during development (Cathala et al., 2000; Clark and Cull-Candy, 2002).

$GABA_A$ receptor-mediated IPSCs tend to decay more slowly than the AMPA conductances. GABAergic synapses from dentate gyrus basket cells onto other basket cells are faster: $\tau_{rise} = 0.3$ ms and $\tau_{decay} = 2.5$ ms (Bartos et al., 2001) than synapses from basket cells to granule cells: $\tau_{rise} = 0.26$ ms and $\tau_{decay} = 6.5$ ms (Kraushaar and Jonas, 2000). Reversal potentials of $GABA_A$ receptor-mediated conductances change with development (Ben-Ari, 2002) and activity (Fiumelli and Woodin, 2007).

Experimentally, accurate measurement of synaptic currents and time constants is difficult because the voltage in dendrites is difficult to control (known as the space-clamp problem; chapter 10, section 3), leading to an overestimate of the rise and decay time constants of the synaptic conductance at distal dendritic locations. Care should therefore be taken to minimize this by optimizing recording conditions, recording from small (i.e., electrically compact) cells, or employing analysis tech-

niques that provide an unbiased estimate of the decay time constant of the synaptic conductance (Häusser and Roth, 1997b; Williams and Mitchell, 2008).

6.2 Implementation Issues

Given the large number of synapses in most network simulations, efficient simulation of synapses is key. For home-brewed simulations, an easy trick is the following: Whereas updating all the synaptic conductances at every time step according to, for instance equation (6.1), is computationally costly, if the postsynaptic neuron contains just a single compartment (e.g., an integrate-and-fire neuron, chapter 7), all synaptic conductances with identical parameters can be lumped together into a total synaptic conductance (Lytton, 1996). This total synaptic conductance g_Σ increases when any of the synapses onto the neuron are activated, i.e., $g_\Sigma = g_\Sigma + g_i$, where i sums over the activated synapses. Only the decay of this summed conductance has to be calculated at each time step dt. For instance, in the case of a single exponential decay, $g_\Sigma(t + dt) = g_\Sigma(t) \exp(-dt/\tau)$, meaning that the computational cost of updating the synaptic conductance is on the order of the number of neurons; i.e., it is comparable to the cost of updating the neuron's membrane potentials only.

Implementation in Simulator Packages

Models of synaptic transmission have also been implemented in neural simulation packages (see the software appendix). Work is under way to improve the accuracy and efficiency of these implementations and, depending on the application, different simulation strategies may be the most accurate and most efficient (Brette et al., 2007). One strategy is to compute the synaptic conductance time courses as the solutions of the corresponding linear differential equations, which can be integrated numerically using discrete time steps, or in some cases can be solved analytically (Destexhe et al., 1998a; Rotter and Diesmann, 1999; Carnevale and Hines, 2006). Instead of analytical solutions, precomputed lookup tables for the synaptic and neuronal dynamics can be also used (Ros et al., 2006).

Another approach is to use event-driven methods, which are particularly efficient in cases that allow an analytical solution for the response of the postsynaptic neuron (Brette, 2006; Carnevale and Hines, 2006; Rudolph and Destexhe, 2006; chapter 7). These algorithms extrapolate the time at which neuron will spike, removing the need for simulating the intermediate time steps. However, if input rates are high, these extrapolations have to be revised frequently, nullifying their benefit. Finally, hybrid strategies that combine time-driven and event-driven methods are available (Morrison et al., 2007). Most synapse models discussed here have also been implemented in hardware, both using analog very large-scale integration (VLSI) (Rasche and

Douglas, 1999; Mira and Álvarez, 2003; Zou et al., 2006; Bartolozzi and Indiveri, 2007) and field-programmable gate arrays (FPGAs) (Guerrero-Rivera et al., 2006).

Axonal, Synaptic, and Dendritic Delays

The postsynaptic response to a presynaptic spike is not instantaneous. Instead, axonal, synaptic, and dendritic delays all contribute to the onset latency of the synaptic current with respect to the time of the presynaptic spike. Since these delays can add up to several milliseconds and thus can be comparable in duration to the synaptic time constant, they can have consequences for synchronization and oscillations (Brunel and Wang, 2003; Maex and De Schutter, 2003; chapter 13, section 3) and the stability of spike timing-dependent plasticity (STDP) in recurrent networks (Morrison et al., 2007). In practice, long delays benefit parallel simulation algorithms (chapter 13, section 6).

6.3 Biophysics of Synaptic Transmission and Synaptic Receptors

After describing these simplified models of synapses, we now focus on the underlying mechanisms of synaptic transmission, which will allow discussion of the more realistic models presented in section 6.4. The precise shape of synaptic events is determined by the biophysical mechanisms that underlie synaptic transmission. Numerous in-depth reviews of synaptic physiology and kinetic models of synaptic receptor molecules exist (Jonas and Spruston, 1994; Jonas, 2000; Attwell and Gibb, 2005; Lisman et al., 2007).

Transmitter Release

The signaling cascade underlying synaptic transmission (figure 6.1) begins with the arrival of the presynaptic action potential in the presynaptic terminal, where it activates various types of voltage-gated ion channels (Meir et al., 1999), in particular, voltage-gated calcium channels. The calcium current through these channels reaches its maximum during the repolarization phase of the action potential as the driving force for calcium ions increases while the calcium channels begin to deactivate (Borst and Sakmann, 1998). This calcium influx leads to a local increase in the intracellular calcium concentration (see chapter 4, section 3 and section 6.5), which in turn triggers the release of neurotransmitter molecules from vesicles, owing either to their full fusion with the presynaptic membrane or the formation of a fusion pore (He et al., 2006).

Transmitter Diffusion

Following its release, the neurotransmitter diffuses in the synaptic cleft. The spatiotemporal profile of transmitter concentration in the synaptic cleft depends on a num-

ber of factors, the first being the rate of release of presynaptic vesicles (figure 6.1). In the absence of full fusion, the release rate of transmitter molecules is also limited by the diameter of the fusion pore (Stiles et al., 1996). The subsequent movement of transmitter molecules is determined by their diffusion coefficient in the synaptic cleft (Nielsen et al., 2004), the geometry of the synapse, and the reuptake of transmitter by transporter molecules in presynaptic cells and glia. Synaptic geometry can change during development (Cathala et al., 2005) and can depend on activity (Genoud et al., 2006), which in turn can change the time course of transmitter in the synaptic cleft. The density of transporter molecules tends to increase during development, speeding up the reuptake of transmitter and sharpening the transmitter transient (Diamond, 2005). The number of transporter molecules available to bind transmitter also depends on past synaptic activity.

Receptor Binding

During the brief transient increase of transmitter concentration in the synaptic cleft, some of the transmitter molecules bind to receptor molecules in the postsynaptic membrane, causing conformational changes that lead to the transient opening of ion channels coupled to the receptors (Madden, 2005; Mayer and Armstrong, 2004; Mayer, 2005, 2006). The kinetics of the postsynaptic receptors is an important determinant of the time course of the synaptic conductance. Functional AMPA, NMDA, and $GABA_A$ receptors are composed of several subunit proteins. The functional properties of a receptor strongly depend on its subunit composition (Geiger et al., 1995; Cull-Candy and Leszkiewicz, 2004; Paoletti and Neyton, 2007). The heterogeneity of receptor subunit composition can explain a large part of the variability in the time course of the synaptic conductance within and between different classes of synaptic connections. Furthermore, during development, a switch in subunit expression occurs in many types of synapses, leading to changes in postsynaptic receptor properties. In particular, such subunit switches tend to accelerate the kinetics of the receptors during development (Feldmeyer and Cull-Candy, 1996; Joshi et al., 2004; T. Takahashi, 2005). Receptor properties can also be changed by various accessory and modulatory subunits. Prominent examples are transmembrane AMPAR regulatory proteins (TARPs) such as stargazin, which modulates AMPA receptor gating and trafficking by distinct domains (Tomita et al., 2005). Thus for a realistic model, the functional properties of synaptic receptors should be studied under conditions that are as close as possible to their native state and environment at the synapse (DiGregorio et al., 2007).

The kinetics of synaptic receptors and their associated ion channels can be described by Markov models (chapter 5, section 5). At any given time, the receptor channel complex is assumed to exist in a given state, such as closed, open, or desensitized. Rate constants determine the transitions between any two of these states.

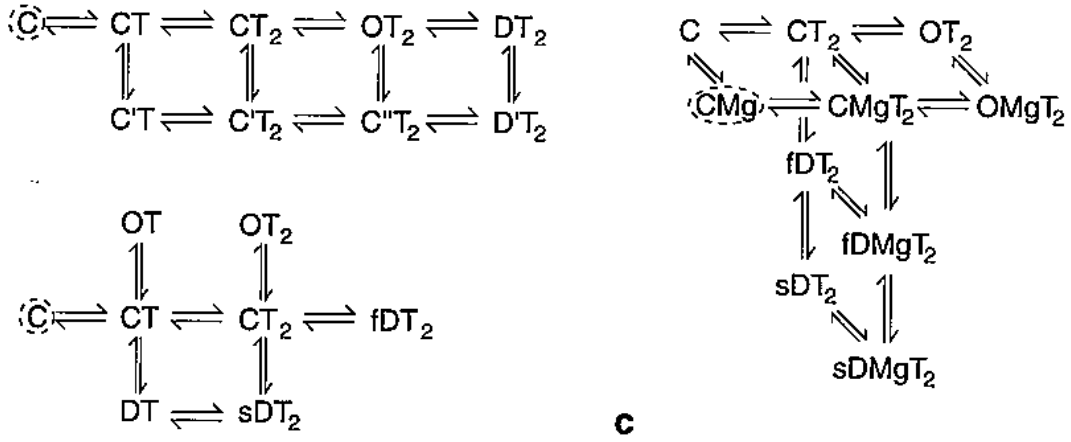

Figure 6.3
Kinetic schemes for common synaptic channels. Closed states are denoted with a C, open states with an O, and desensitized states with a D. Primes are used to distinguish otherwise identical states. The transmitter is denoted by T. A circled state denotes the state at rest, in the absence of a transmitter. (a) AMPA receptor kinetic model after DiGregorio et al. (2007). Two transmitter molecules T need to bind for the channel to open. (b) $GABA_A$ receptor kinetic model after Pugh and Raman (2005). Note that there are two open states in this case. The desensitized states are split into slow (sD) and fast (fD) ones. (c) NMDA receptor kinetic model after Kampa et al. (2004). The model includes the kinetics of magnesium (Mg) binding. For simplicity, the binding with both glutamate molecules has been captured in a single transition. Again there are both slow and fast desensitized states.

State transitions involving the binding of a transmitter molecule to the receptor are described by rate constants that are proportional to the transmitter concentration. The rate constants are free parameters in these models, which need to be extracted from experimental data. Except for the simplest Markov models with only two or three states, which might not describe the synaptic receptors very well, the number of rate constants and thus the number of free parameters is significantly larger than the number of free parameters in simple functions describing synaptic conductance kinetics (section 6.1). It is usually necessary to expose receptors to a number of protocols involving both short and long pulses of transmitter concentration (e.g., Häusser and Roth, 1997a) to adequately constrain a Markov model of their kinetics. A number of Markov models for AMPA receptors from different types of neurons have been obtained in this way (Nielsen et al., 2004). Figure 6.3a shows a kinetic model of synaptic AMPA receptors in cerebellar granule cells (DiGregorio et al., 2007) and table 6.1 provides the rate constants for the models. Kinetic models of NMDA receptors with a slow component of the magnesium unblock (Kampa et al., 2004; Vargas-Caballero and Robinson, 2003, 2004; figure 6.3c) can be useful for simulations of NMDA receptor-dependent synaptic plasticity (section 6.7).

In order to use Markov models of synaptic receptors, a model of the time course of the transmitter concentration in the synaptic cleft is needed to drive the Markov model. Models of transmitter diffusion in detailed synaptic geometries (section 6.5) may provide fairly accurate predictions of the time course of transmitter concentration, but are computationally very expensive. However, because the transmitter

Table 6.1
Rate constants for the models in figure 6.3

Transition	Forward	Backward
	AMPA	
C-CT	13.66 $mM^{-1}ms^{-1}$	8.16 ms^{-1}
CT-CT_2	6.02 $mM^{-1}ms^{-1}$	4.72 ms^{-1}
CT-C′T	0.11 ms^{-1}	0.1 ms^{-1}
C′T-C′T_2	13.7 $mM^{-1}ms^{-1}$	1.05 ms^{-1}
C′T_2-C″T_2	0.48 ms^{-1}	0.98 ms^{-1}
CT_2-OT_2	17.2 ms^{-1}	3.73 ms^{-1}
C″T_2-D′T_2	10.34 ms^{-1}	4 ms^{-1}
CT_2-C′T_2	2 ms^{-1}	0.19 ms^{-1}
OT_2-C″T_2	0.0031 ms^{-1}	0.0028 ms^{-1}
OT_2-DT_2	0.11 ms^{-1}	0.09 ms^{-1}
DT_2-D′T_2	0.0030 ms^{-1}	0.0013 ms^{-1}
	$GABA_A$	
C-CT	0.04 $\mu M^{-1}ms^{-1}$	2 ms^{-1}
CT-OT	0.03 ms^{-1}	0.06 ms^{-1}
CT-DT	0.000333 ms^{-1}	0.0007 ms^{-1}
CT-CT_2	0.02 $\mu M^{-1}ms^{-1}$	4 ms^{-1}
CT_2-OT	10 ms^{-1}	0.4 ms^{-1}
CT_2-sDT_2	1.2 ms^{-1}	0.006 ms^{-1}
CT_2-fDT_2	15 ms^{-1}	0.15 ms^{-1}
DT-sDT_2	0.015 $\mu M^{-1}ms^{-1}$	0.007 ms^{-1}
	NMDA[a]	
C-CT_2	10 $\mu M^{-1}s^{-1}$	5.6 s^{-1}
CMg-CMgT_2	10 $\mu M^{-1}s^{-1}$	17.1 s^{-1}
CT_2-OT_2	10 s^{-1}	273 s^{-1}
CMgT_2-OMgT_2	10 s^{-1}	548 s^{-1}
CT_2-fDT_2	2.2 s^{-1}	1.6 s^{-1}
CMgT_2-f$DMgT_2$	2.1 s^{-1}	0.87 s^{-1}
fDT_2-sDT_2	0.43 s^{-1}	0.50 s^{-1}
f$DMgT_2$-s$DMgT_2$	0.26 s^{-1}	0.42 s^{-1}
O-OMg (at +40 mV)	0.05 $\mu M^{-1}s^{-1}$	12,800 s^{-1}
x-xMg (at +40 mV)	50.10^{-6} $\mu M^{-1}s^{-1}$	12.8 s^{-1}

[a] See also http://senselab.med.yale.edu/modeldb, model = 50207.

transient is much faster than the receptor dynamics, a brief square pulse or a single-exponential decay suffices (Destexhe et al., 1998a).

Second-Messenger Synapses

In the preceding discussion, the transmitter binds to the ion channels directly, so-called ionotropic receptors. However, this is not always the case. In second-messenger or metabotropic receptors (Coutinho and Knöpfel, 2002), the neurotransmitter binds to a receptor that activates an intermediate G-protein, which in turns binds to a G-protein-gated ion channel and opens it. As a result of the intermediate cascade, the synaptic responses of second-messenger synapses are usually slower, but they can also be very sensitive and highly nonlinear. For the same reason, unified models of second-messenger synapses are rare and can display a rich behavior. The best-known examples of these synapses are the metabotropic glutamate receptors and the inhibitory receptor $GABA_B$. In the case of $GABA_B$, the inhibitory current becomes disproportionally stronger with multiple events (Destexhe et al., 1998a). The nonlinearity of the mGluR receptor in retinal bipolar cells has, for instance, been proposed to filter out photoreceptor noise (van Rossum and Smith, 1998). Finally, mGluR receptors have also been found presynaptically (T. Takahashi et al., 1996; R. J. Miller, 1998).

6.4 Modeling Dynamic Synapses

Many of the biophysical mechanisms involved in synaptic transmission are use dependent (Zucker and Regehr, 2002). For example, residual elevations of the presynaptic calcium concentration that are due to a previous action potential can increase the probability of subsequent transmitter release. An increase in the synaptic response to successive stimuli is called synaptic facilitation. On the other hand, depletion of the pool of readily releasable vesicles can cause a decrease of the synaptic response to successive stimuli, called short-term synaptic depression (to distinguish it from long-term synaptic depression, LTD, the counterpart of long-term potentiation, LTP). Depression and facilitation of synaptic currents can also have postsynaptic components (Heine et al., 2008). Cumulative desensitization of postsynaptic receptors can contribute to synaptic depression, while increased occupancy of transporters can lead to a prolonged presence of transmitter molecules in the synaptic cleft and a facilitation of synaptic responses.

Short-term synaptic plasticity is a major determinant of network dynamics. It can provide gain control, underlie adaptation and detection of transients, and constitute a form of short-term memory (Abbott and Regehr, 2004; chapter 13, section 3). The characteristics of short-term synaptic plasticity depend on (and can be used to define) the type of synaptic connection in a neural circuit (Silberberg et al., 2005). A number

of functional consequences of short synaptic dynamics have been suggested: temporal filtering (Puccini et al., 2007), gain adaptation (Abbott et al., 1997), decorrelation of inputs (Goldman et al., 2002), working memory (Mongillo et al., 2008), and adaptive visual processing (van Rossum et al., 2008).

The amplitude and time constants of synaptic depression and facilitation, which can be determined experimentally using trains of synaptic stimuli, are free parameters of simple phenomenological models of short-term synaptic plasticity (Abbott et al., 1997; Markram et al., 1998; Tsodyks et al., 2000). These models are a good approximation of the short-term dynamics of many types of synapses and can be implemented efficiently.

We present here the model of Tsodyks and Markram as described in Tsodyks et al. (1998, 2000). In this model, the "resources" of the synapse that provide the synaptic current or conductance can exist in one of three states: the recovered or resting state, with occupancy x; the active or conducting state, y; and an inactive state, z. At any given time

$$x + y + z = 1. \tag{6.13}$$

A fourth state variable, u, describes the "use" of synaptic resources in response to a presynaptic action potential arriving at time $t = t_0$. Its dynamics is given by

$$\frac{du}{dt} = -\frac{u}{\tau_{\text{facil}}} + U(1-u)\delta(t-t_0), \tag{6.14}$$

so u is increased by $U(1-u)$ with each action potential and decays back to zero with a time constant τ_{facil}. This u drives the dynamics of the other three state variables according to

$$\frac{dx}{dt} = \frac{z}{\tau_{\text{rec}}} - ux\delta(t-t_0) \tag{6.15}$$

$$\frac{dy}{dt} = -\frac{y}{\tau_{\text{decay}}} + ux\delta(t-t_0) \tag{6.16}$$

$$\frac{dz}{dt} = \frac{y}{\tau_{\text{decay}}} - \frac{z}{\tau_{\text{rec}}}, \tag{6.17}$$

where τ_{rec} is the time constant of recovery from depression and τ_{decay} (corresponding to τ in equation 6.1) is the time constant of decay of the synaptic current or conductance, which is proportional to y.

Typical observed time constants for recovery are between 100 and 1,000 ms in vitro. The time constants and magnitude of synaptic depression in vivo have not been clearly established, however. With background activity, synapses might already

be in a somewhat depressed state before stimulation begins, making depression less pronounced than in a slice preparation, for which background activity is commonly absent (Reig et al., 2006). Furthermore, synaptic depression is also known to depend on the specific synaptic connection (Thomson and Lamy, 2007) and brain area (Wang et al., 2006). Models with multiple time constants have also been proposed (Varela et al., 1997) and biophysical models have been made (Hennig et al., 2008).

An efficient scheme to simulate synaptic depression is discussed in Morrison et al. (2008). For an example implementation in NEURON, see model 3815 in ModelDB (http://senselab.med.yale.edu/ModelDb); other efficient implementations of related models can be found in Giugliano et al. (1999) and Giugliano (2000). A hardware implementation in analog VLSI is described by Bartolozzi and Indiveri (2007).

6.5 Stochastic Models of Synaptic Transmission

The descriptions of synaptic transmission we have discussed so far are deterministic. However, synaptic responses show considerable trial-to-trial variability, owing to the stochastic nature of many steps in the signaling cascade underlying synaptic transmission (for a review, see Faisal et al., 2008).

Sources of variability have been studied in nearly all components of the cascade and include variations in the waveform of the presynaptic action potential and stochastic gating of presynaptic calcium channels, which lead to variability in the amount of calcium entering the presynaptic terminal in response to a presynaptic action potential; randomness of the diffusion of the individual calcium ions; stochastic gating of the release mechanism for presynaptic vesicles; variability across vesicles in the number of transmitter molecules contained in or released from a vesicle, owing to variations in vesicle size, the degree of filling with transmitter, and incomplete emptying in the absence of full fusion; variability in the location of the release site in the presynaptic membrane with respect to the postsynaptic density; random diffusion of transmitter molecules in the synaptic cleft; stochastic gating of the postsynaptic receptors; and changes in the number of available postsynaptic receptors that are due to lateral diffusion of receptors in the postsynaptic membrane (Heine et al., 2008).

In principle, a composition of biophysically realistic quantitative descriptions of the stochasticity of all these steps can be put together, but this would result in a complicated model with many parameters that are difficult to estimate from available data. In practice it may be more useful to represent several steps in a simpler, phenomenological stochastic model. Here we focus on simple stochastic descriptions of transmitter release (for a biophysical model of presynaptic calcium dynamics, see Meinrenken et al., 2002), stochastic modeling of transmitter diffusion (see also chapter 3), and stochastic models of channel gating.

Stochastic Models of Vesicle Release

The description of synaptic potentials and synaptic currents as a sum of probabilistically generated "quantal components" has its origin in the work of del Castillo and Katz (1954) at the neuromuscular junction. More recently, it has been used to interpret the fluctuations of EPSP amplitudes measured in paired recordings from synaptically connected neurons in the central nervous system (Thomson et al., 1993; Markram et al., 1997; Brémaud et al., 2007). In its simplest version, the synapse is described as an arrangement of n independent release sites, each of which releases a quantum of transmitter with a probability p in response to a presynaptic action potential. Each released quantum of transmitter generates a contribution of size q to the postsynaptic response r (which can be a synaptic conductance, current, or postsynaptic potential amplitude). Therefore r follows a binomial distribution and the mean response $\langle r \rangle$ is

$$\langle r \rangle = npq. \tag{6.18}$$

Individual responses can be simulated using binomially distributed random numbers. If n is low, this can be done by generating n random deviates uniformly distributed between zero and one. The number of deviates smaller than p gives the synaptic amplitude after multiplication by q. By using different values of p_i and q_i, this scheme can be generalized to the case that different release sites (indexed by i) have different release probabilities p_i and quantal sizes q_i.

Typical values for p are between 0.1 and 0.5 but can vary widely, whereas n typically ranges between 3 and 20 (Markram et al. 1997; Brémaud et al., 2007). The number of anatomical contacts is probably close to n, but because combining anatomy and physiology in a single experiment is difficult, a precise quantification is currently lacking.

For a model that combines stochastic release and short-term plasticity, see Maass and Zador (1999). It is generally believed that the stochastic release of vesicles is a large source of variability in the nervous system. Whether this variability is merely the consequence of the underlying biophysics or has some functional role is a topic of active debate.

Stochastic Models of Transmitter Diffusion

A simulator for the stochastic simulation of transmitter diffusion and receptor binding is MCell (see the software appendix). MCell simulates diffusion of single molecules and the reactions that take place as transmitter molecules bind to receptors and transporters, which can be used to quantify the different sources of variability (Franks et al., 2003; Raghavachari and Lisman, 2004).

Stochastic Models of Receptors

A stochastic description of the stochastic opening of the postsynaptic receptors is straightforward once a Markov model has been formulated. Instead of using the average transition rates in the state diagram, at each time step the transitions from one state to another are drawn from a binomial distribution, with a probability p equal to the transition rate per time step, and n equal to the number of channels in the state at which the transitions are made. The fewer receptors there are in the postsynaptic membrane, the more pronounced the fluctuations around the average behavior will be. The typical number of postsynaptic receptors is believed to be in the range of 10 to 100. Compared with the other sources of variability, the noise from stochastic opening of the receptor channels is usually minor (van Rossum et al., 2003). Nevertheless, the fluctuations across trials can be used to determine the unitary conductance of the receptors using so called nonstationary noise analysis (Hille, 2001). Computationally, these simulations are expensive because the number of transitions is assumed to be small in the simulation, whereas the transition rates can be high, necessitating a very small time step.

6.6 Modeling Synaptic Learning Rules

One of the central hypotheses in neuroscience is that learning and memory are reflected in the weight of synapses. Many experiments and models have studied therefore how synapses change in response to neural activity, so-called activity-dependent synaptic plasticity. Some models have as their aim the construction of learning rules so that the network performs a certain task, such as learning input-output associations (for instance, using backpropagation), independent component analysis, or achieving sparse codes. Because the links between these models and the physiology are often tentative, we will not describe them here. Another class of models, discussed here, uses a phenomenological approach and implements biologically observed learning rules to examine their functional consequences.

The biological pathways underlying synaptic plasticity are only just starting to be understood, but it clear that they contain many ingredients and regulation mechanisms. Although efforts are being made to model at this level (chapter 3), for network studies one often prefers a simpler model. This separation of levels of complexity is often desirable conceptually, but also from a computational perspective. In plasticity studies one is often interested in a network's properties as they evolve over longer periods of time or when many stimuli are presented. This means that simulation studies of learning are computationally particularly expensive and require efficient algorithms.

The fundamental experimental finding is that brief exposure to high pre- and postsynaptic activity causes long-lasting increases in synaptic strength, which can persist up to months in vivo (Bliss and Lomo, 1973). This finding is consistent with Hebb's hypothesis (Hebb, 1949) and is called Hebbian learning. This phenomenon is known as LTP. Similarly low, but nonzero, levels of activity can cause long-lasting weakening of synapses, LTD. Consistent with most experiments, increases and decreases in synaptic efficacy in most models are implemented through changes in the postsynaptic conductance $\bar{g}_{\text{syn}}$, although in some studies evidence for changes in the release probability was found and has been included in models (Tsodyks and Markram, 1997; Maass and Zador, 1999).

Rate-Based Plasticity

In an effort to condense the experimental data on plasticity, early plasticity models used often a rate-based formulation, which, for instance, takes the form (Sejnowski, 1977):

$$\Delta w_{ij} = \varepsilon(r_i - a)(r_j - b), \tag{6.19}$$

where r_i is the presynaptic firing rate, r_j is the postsynaptic firing rate, w_{ij} is the synaptic weight connecting the neurons, and a and b are constants. Finally, the proportionality constant ε is often taken to be a small number, ensuring that the synaptic weights change only slowly. The rates are assumed to be averaged over times longer than any single neuron dynamics (such as spikes) but shorter than the stimulus dynamics. Such a learning rule, for instance, can be used to train networks receiving sensory input in an unsupervised manner.

It is not difficult to see that this learning rule diverges, however, because once a synapse becomes stronger, it will evoke a higher postsynaptic activity, which leads to a further increase in its strength, etc. A variety of solutions have been proposed to deal with this problem. These include imposing maximum and minimum weights, normalizing the sum of all the weights coming into a neuron, while the Bienenstock-Cooper-Munro (BCM) rule adjusts the thresholds of LTP and LTD as a function of average postsynaptic activity (Bienenstock et al. 1982; Dayan and Abbott, 2002). The precise solution strongly affects the resulting behavior of the learning rule while at the same time experimental data on this issue are largely lacking. Despite this uncertainty, or maybe owing to the freedom it allowed, many rate-based plasticity models have been used successfully to describe memory models (Bienenstock et al., 1982; K. D. Miller, 1996; Miikkulainen and Sirosh, 2005).

Spike Timing-Dependent Plasticity

Changes in synaptic weight depend not only on mean firing rates but also on the precise temporal order of pre- and postsynaptic spikes, a phenomenon known as STDP

(Abbott and Gerstner, 2004; Caporale and Dan, 2008). Given a spike at time t_i in the presynaptic neuron and at time t_j in the postsynaptic neuron, a simple description of STDP is

$$\Delta w_{ij} = \varepsilon \operatorname{sign}(t_i - t_j) \exp(-|t_i - t_j|/\tau_{\mathrm{STDP}}), \tag{6.20}$$

where τ_{STDP} is the time window for spike pair interaction, some 20 ms. Note that the weight change is discontinuous when $t_i = t_j$.

However, the apparent simplicity of the STDP rule is a bit misleading because for an actual implementation, additional specifications are needed. First, without any further constraints, weights will diverge as more and more spike pairs are encountered. As for rate-based plasticity rules, bounds can be imposed. These can be hard bounds that simply cap the maximal weight, or softer bounds that, for instance, reduce the amount of potentiation as the weight increases. In addition, homeostatic mechanisms can be included that modify the learning rules based on the total postsynaptic activity. Second, one needs to define which spike pairs contribute to weight changes. For instance, what happens if a presynaptic spike is followed by two postsynaptic spikes; do both contribute to a weight modification? Such rules can be classified and analyzed formally to some extent (Burkitt et al., 2004).

Although in equation (6.20) the STDP rule is independent of the pre- and postsynaptic rate, experiments show that higher pairing frequencies usually cause LTP and lower frequencies cause LTD. As long as there is no experimental evidence that STDP and rate-based learning are separate plasticity mechanisms, it is convenient to unify them in a single framework. Unified models of STDP and rate-based learning that even include BCM-like plasticity have been created by allowing higher-order interactions between spikes (Pfister and Gerstner, 2006).

This raises the question of whether the temporal character of STDP matters at all or is simply a side effect of a biological implementation of rate-based learning. Although this issue has not been settled yet, there is evidence that some perceptual learning shares properties with STDP (Dan and Poo, 2006) and that some plasticity phenomena can only be explained by using STDP (Young et al., 2007).

Analysis of STDP in networks is difficult because of the mutual interaction between the spike patterns in the network, which will modify the synapses, and the plasticity, which will modify the activity patterns. Even creating a stable asynchronous state in a network with STDP is challenging but possible (Morrison et al., 2007).

Biophysical Models of Long-Term Potentiation

The molecular biology of LTP is quite complicated and involves numerous pathways. LTP is critically dependent on calcium influx in the postsynaptic membrane that activates CaMKII (Lisman et al., 2002). The calcium influx is strongly depen-

dent on spike sequence and has been used as a basis for STDP (Shouval et al., 2002; Badoual et al., 2006). Experiments have further distinguished between different phases of plasticity, so-called early LTP (lasting a few hours) and late LTP (perhaps lasting indefinitely). In particular, the stability of LTP has received attention from modelers (Graupner and Brunel, 2007; Lisman and Raghavachari, 2006).

Again, synapses of different neurons obey different learning rules and even on a given neuron, synapses at different dendritic locations can have distinct plasticity rules (Sjöström et al., 2008). Thus far this level of complexity has largely been ignored in functional models.

6.9 Conclusions

We have presented synaptic models at various levels of physiological detail and realism. We started with some quite simple formulations that nevertheless provide decent models for the synaptic current. Increases in computer speed and increased understanding of neural transmission have made more and more complex models possible. The researcher will need to consider a tradeoff between complex models and simpler models that may ignore subtleties. However, a simple heuristic model is not necessarily inferior, because it might actually do a better job in describing the physiology than a complicated model with incorrect parameters.

Unless biophysical mechanisms of synaptic transmission themselves are the subject of study, mechanistic detail is usually not needed. Experimental data that constrain all parameters of these phenomenological models, such as voltage-clamp recordings of synaptic current waveforms, are more likely to be available than full experimental characterizations of the functional properties of the molecules and the biophysical mechanisms involved. Furthermore, complex models not only require more computer time but also more time to set up, verify, tune, and analyze. An informed choice of model will depend on the question that is being asked. No matter what model is used, parameter values should be considered carefully. For instance, the strong temperature dependence of gating kinetics implies that data recorded at room temperature should not simply be plugged into an in vivo model.

Recent years have also seen increased understanding of issues such as long-term and short-term synaptic plasticity, receptor diffusion, and subunit composition, to name but a few. Unfortunately for the modeler, the known diversity among synapses and their properties has also increased. The number of variations in synaptic subunit composition, modulation (not discussed here), and long- and short-term dynamics is ever increasing, and there is no reason to expect a slowdown in this trend. The rules that underlie this diversity are so far largely unknown, so intuition and exploration are required from the modeler.